Escola de Camins
Escola Tècnica Superior d'Enginyeria de Camins, Canals i Ports
UPC BARCELONATECH

TREBALL FINAL DE GRAU

Flexoelectricity in nanobeams under torsion

Treball realitzat per:
Jordi Moliner Martínez

Dirigit per:
Irene Arias & Amir Abdollahi

Grau en:
Enginyeria Civil

Barcelona, 23 de juny del 2016.

Departament d'Enginyeria Civil i Ambiental

Abstract

Flexoelectricity in nanobeams under torsion

Jordi Moliner Martínez

Electromechanical couplings are essential in many technological fields. These materials are capable of creating an electric field when being deformed but also to deform when subjected to an electric field. Piezoelectricity is usually the first word that comes into our mind when talking about electromechanical coupling. Nonetheless, during the 60s, a new electromechanical coupling was discovered: flexoelectricity. Flexoelectricity is a universal property of all dielectrics by which they generate a voltage in response to an inhomogeneous deformation. It couples polarization and strain gradient and it exists in a wide variety of materials, being most noticeable for nanoscale objects, where strain gradients are higher.

Polarization and strain gradient are related by a flexoelectric coefficient. Self-consistent numerical solutions of the flexoelectric governing equations are fundamental to understanding flexoelectricity and interpreting characterization experiments. Several studies have focused on estimating these coefficients under bending and compression. Nevertheless, flexoelectricity under torsion has not been addressed so far. One possible reason is that linear isotropic elasticity predicts a strain-gradient field producing no polarization in a material with cubic flexoelectric symmetry aligned with the axis of the rod. This is the case even for non-circular cross-sections when uniform warping is assumed. However, deviations from this ideal theory may mobilize flexoelectricity.

In this work, we explore this possibility by studying the flexoelectric response of nanobeams under torsion both analytically and computationally. We first show with a simplified analytical model that a polarization can indeed be obtained in a truncated cone under torsion. The coupled governing equations of flexoelectricity are then solved in the same geometry. Since these equations involve high-order spatial derivatives, standard C^0 finite elements cannot be used. Here we resort to a method based on smooth shape functions, thus providing both continuity and derivability to simulate the flexoelectric effect. Both analytical and numerical results are compared and discussed. Finally, other geometries are analyzed and compared among them using numerical simulations to evaluate the flexoelectric response.

Flexoelectricity in nanobeams under torsion

Jordi Moliner Martínez

Flexoelectricity → electromechanical coupling

$$P_i = \mu_{ijkl} \frac{\partial \varepsilon_{jk}}{\partial x_l}$$

- Relation between strain gradient & polarization
- Nanoscale systems induce larger strain gradients
- Presence in any crystalline material

Characterization of the flexoelectric tensor μ_{ijkl}

Reduced to 3 components for cubic symmetry materials

- Longitudinal: μ_{1111}
- Transversal: μ_{1122}
- Shear: μ_{1212}

Setups to characterize μ_{ijkl}

- μ_{1111} → cantilever beam under flexion
- μ_{1122} → truncated pyramid under compression

But:

- μ_{1212} → no setups until the moment

Torsion could induce a shear strain gradient

Need to explore geometries to obtain P analytically

The elastic problem is solved for:

- Cylindrical bar: $\partial \varepsilon_{jk} / \partial x_l = 0 \rightarrow P = 0$
- Truncated cone: $\partial \varepsilon_{jk} / \partial x_l \neq 0 \rightarrow P \neq 0$

Polarization is obtained when a torque is applied on the free end of a truncated cone

But the elastic and the electric problems are uncoupled

↓

A certain error is produced

$P_{max\ ,analytically} = 0.0434\ C/m^2$

Numerical methods are needed to solve the coupled problem accurately

$\partial \varepsilon_{jk} / \partial x_l$ → need to compute 2nd derivatives of the displacement field → cannot use traditional FEM

Local *maximum - entropy* scheme with $\mathcal{C}^\infty$ smooth functions is used to obtain P

$P_{max\ ,numerically} = 0.0323\ C/m^2$

Comparison of results:

$P_{max\ ,numerically} \cong P_{max\ ,analytically}$

In both cases P is maximum where the torque is applied

Analytical solution produces small error for this case

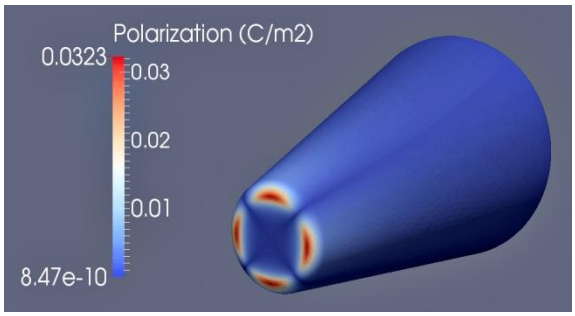

Other geometries are studied:

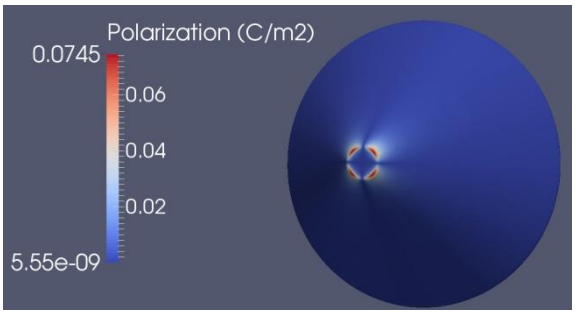

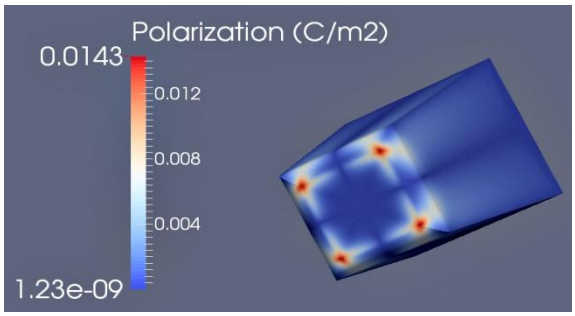

Error of one order of magnitude between analytical and numerical solutions for the plate truncated cone

↓

To measure polarization accurately with general geometries, numerical method is needed

The maximum value of P is obtained for a plate truncated cone → ideal candidate for experimental configuration

Acknowledgements

Firstly, I would like to thank Irene and Amir for the support during the development of this work and for the uncoutable meetings to solve all kind of doubts with empathy, patience and a smile.

Secondly, I would like to thank my sister, my mother, my father, my grandparents and every member of my family the support during these four years, especially during the first one, when things seemed terribly bad. They encouraged me to believe and not to fall. Without you I would not have made it until today.

Finally, I would like to thank Montse for being my confidant through thick and thin. By your side I am always strong and I can always carry on even under the worst circumstances thanks to your smile and your love.

Contents

List of Figures

List of Tables

1 Introduction

1.1 Field of study

Electromechanical coupling, i.e. the coupling between electrical and mechanical properties, is present in a large variety of materials. Piezoelectricity is the first word that comes up to our minds when mentioning electromechanical coupling. Only a small group of materials (those which are non-centrosymmetric) are piezoelectric, which means they are capable of developing polarization when a homogeneuos deformation is applied and viceversa. Nonetheless, there are many other materials in which electromechanical coupling exists and they are not necessarily following the rules of piezoelectricity. Then, what phenomenon induces polarization when these materials are deformed? Flexoelectricity.

Flexoelectricity is a universal property of all dielectrics by which they generate a voltage in response to a strain gradient and viceversa, rather than polarization and strain as in piezoelectricity (Kogan, 1964 and Tagantsev, 1986). It is considered to be an essential electromechanical coupling in non-piezoelectric materials (Zhu et al., 2006).

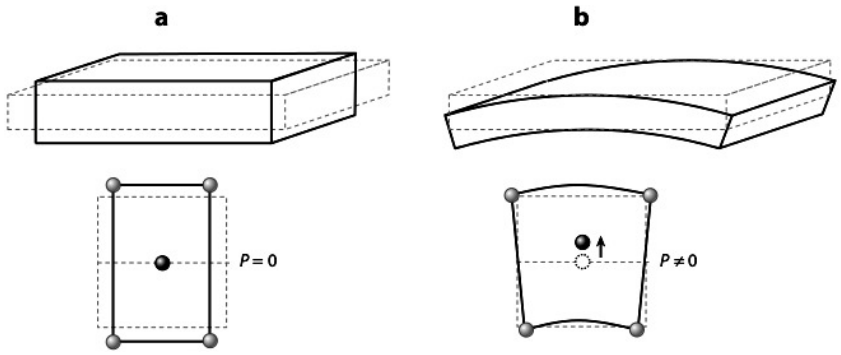

Figure 1: Atomic mechanism of flexoelectricity: (a) Uniform strain that does not break inversion symmetry so it cannot create polarization in a centrosymmetric material. (b) Strain gradient that breaks inversion symmetry and leads to relative displacements of the centers of both negative and positive charges, inducing polarization in any material (Zubko et al., 2013).

While piezoelectricity is induced by a homogeneous deformation, flexoelectricity is induced by a strain gradient or, in other words, an inhomogeneous deformation. Thus, flexoelectricity effects are considerably higher in nanoscale systems than in macroscale systems because strain gradients are inversely proportional to the element size. This is

a situation that civil engineers are not used to dealing with because most of the time inhomogeneous deformations are avoided by all means since they lead to stress concentrations and damage. Now it is time to face a problem the other way around, trying to maximize heterogeneous strain in order to obtain as much polarization as possible due to the flexoelectric effect.

Furthermore, only crystalline structures with no inversion symmetry (non-centrosymmetric) can develop piezolectricity, whereas flexoelectricity can be induced in any crystalline material regardless the atomic bonding configuration (Resta, 2010 and Hong and Vanderbilt, 2011). This property widens the alternative of materials that can produce polarization when being non-uniformly deformed. For a detailed schematic, see Fig. (1).

These differences between both phenomena are crucial to understand the importance of flexoelectricity and the impact of recent studies related to it. The flexoelectric effect can be exploited in any dielectric material, regardless if it is piezoelectric or not, which makes it universal. Despite that inducing a strain gradient is more difficult than inducing a simple deformation, flexoelectricity has recently gained attention due to the current popularity of nanotechnology and the continuous development of nanomaterials (Nguyen et al., 2013). Research on this field is expected to grow in the near future, widening the applications of flexoelectricity.

The fields of study related to flexoelectricity are extensive. Recent works have shown that this phenomenon may be present in hair cells (Nguyen et al., 2013), biological membranes (Petrov, 2002), viruses (Kalinin et al., 2006), soft materials such as liquid crystals (Petrov, 1975) or even graphene (Kalinin and Meunier, 2008), among many others.

Polarization is proportional to the strain gradient and to the flexoelectric coefficient. Thus, the larger the values of strain gradient and/or flexoelectric coefficient are, the more polarization is induced. It has been found that flexoelectric coefficients are particularly large in materials with high dielectric constants, such as ferroelectrics (Ma and Cross, 2006 and Cross, 2006). To quantify flexoelectricity in experiments it is essential to use materials with large flexoelectric coefficients in order to measure a noticeable value of polarization.

Thus, flexoelectricity is used in a continuum setting as a linear relation between polarization and strain gradients characterized by a forth-rank tensor.

The fundamental equation of flexoelectricity can be expressed as:

$$P_i = d_{ijk}\sigma_{jk} + \mu_{ijkl}\frac{\partial \varepsilon_{jk}}{\partial x_l}\,, \tag{1}$$

where P_i is the polarization, d_{ijk} is the coefficient of direct piezoelectric effect, σ_{jk} is the applied stress, μ_{ijkl} is the fourth-order tensor of flexoelectricity and $\partial\varepsilon_{jk}/\partial x_l$ is the strain gradient.

For centrosymmetric materials for which piezoelectric effects are absent, Eq. (1) becomes:

$$P_i = \mu_{ijkl}\frac{\partial \varepsilon_{jk}}{\partial x_l}\,. \tag{2}$$

The polarization due to the strain gradient is proportional to a fourth-order tensor of 54 different components, commonly represented as μ_{ijkl}. For materials with cubic symmetry, these 54 different components are reduced to 3, which are related to longitudinal, transversal and shear stresses, as presented in Table (1).

Stress	$\boldsymbol{\mu_{ijkl}}$
Longitudinal	μ_{1111}
Transversal	μ_{1122}
Shear	μ_{1212}

Table 1: Flexoelectric coefficients for each type of stress.

Recent studies have focused on obtaining the μ_{1111} and μ_{1122} coefficients. The most common setups to characterize these coefficients are the cantilever beam (Abdollahi et al., 2014) and the truncated pyramid (Abdollahi et al., 2015). Intuitively, the third flexoelectric coefficient μ_{1212} could be characterized with a torsion setup. Nonetheless, there are not any studies of flexoelectricity in beams under torsion except (Zhang et al., 2013), but the shear flexoelectric coefficient μ_{1212} is not characterized. A possible explanation is that the theory of elasticity predicts a strain gradient field which does not induce polarization in a material with flexoelectric symmetry aligned with the longitudinal axis of the beam. The same problem happens with non-circular sections if uniform warping is assumed (Sokolnikoff, 1948).

1.2 Objectives

The objective of this work consists on exploring the possibility of using torsion to obtain polarization that could be measured in a experiment and therefore characterize the μ_{1212} coefficient. Firstly, several configurations of beams will be studied following analytical methods to check whether they are capable of inducing polarization. Secondly, the flexoelectric coupled problem will be solved numerically using a meshless method with smooth basis functions to deal with high order spatial derivatives. Then, both analytical and numerical results will be compared. Finally, other configurations and geometries will be explored to maximize the polarization. One of these configurations could be eventually studied in an experiment and therefore the μ_{1212} coefficient could be estimated.

The structure of the work is as follows. In Section (2), the state of the art is developed and the current situation of the flexoelectric fields is presented as well as the most noticeable setups that have been carried out until the moment. In Section (3), the methodology used in this work is described. The analytical method to obtain a flexoelectric effect under a torque applied on a truncated cone is introduced in Section (3.1) and the numerical method used to obtain a flexoelectric response is explained in Section (3.2). In Section (3.3), both methods are compared to check whether their solutions are consistent or not. In Section (4) the results are discussed and other geometries apart from the truncated cone are analyzed and compared. Finally, in Section (5) the main conclusions of this work are presented as well as the directions of future work that could be followed in order to expand the research on flexoelectricity.

2 State of the art

Several studies on flexoelectricity have been carried out during the last years. Nevertheless, the μ parameter characterization has not always been accurate enough. From Eq. (2) it is possible to see that a strain gradient produces an electric polarization and viceversa. It is not possible to calculate separately the elastic and the flexoelectric problems because both phenomena are coupled.

This situation can be explained with the direct and converse flexoelectric effect. For the direct effect, in the absence of an electric field, a strain gradient induces a homogeneous polarization. Nevertheless, for the converse effect, in a mechanically free sample, a homogeneous electric field does not cause a strain gradient or any other linear mechanical response (Zubko et al., 2013).

Solving the coupled problem with analytical methods is complex. An alternative to proceed is to neglect this coupling effect and introduce the solution of the elastic problem in the equation of flexoelectricity, but taking into account that some error will be produced. A few studies in the last years followed the already mentioned proceeding, which may imply errors of several orders of magnitude between theoretical and experimental estimations depending on features such as the geometry of the problem (Zubko et al., 2007).

The most common setups to characterize the longitudinal and the transversal flexoelectric coefficients are detailed below. Then, other studies related to shear flexoelectricity are introduced.

2.1 Cantilever beam setup

This setup is a typical 2D study of the flexoelectric effect. It consists on a cantilever beam under a mechanical point load F at the non-fixed end. Two different cases of study are analyzed: the first case consists on an open circuit configuration where the electric potential is set to zero at the fixed end, whereas the second case consists on a closed circuit configuration where the electric potential is fixed to zero at the top with an electrode at the bottom (Abdollahi et al., 2014). In Fig. (2), a detailed schematic of this setup is presented.

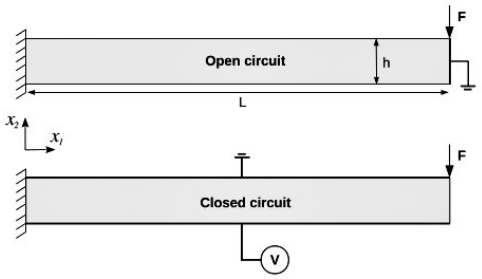

Figure 2: Cantilever beam setup (Abdollahi et al., 2014).

Therefore, in this first setup the methodology to obtain values of the longitudinal coefficient μ_{1111} is analyzed. The value of this coefficient is estimated to be between 1 and $100\,\mu C/m$ for BST (Zubko et al., 2013). This coefficient relates the flexoelectric response after applying a bending load, which induces a strain gradient on the cantilever beam.

2.2 Truncated pyramid setup

This setup is a 3D study of flexoelectricity, which makes it more complex than the setup introduced in Section (2.1). It consists on a truncated pyramid under a mechanical load F, uniformly distributed at the top and bottom surfaces, where the electric potential is zero at the bottom and constant but unknown at the top (Abdollahi et al., 2015). In Fig. (3), a detailed schematic of this setup is presented.

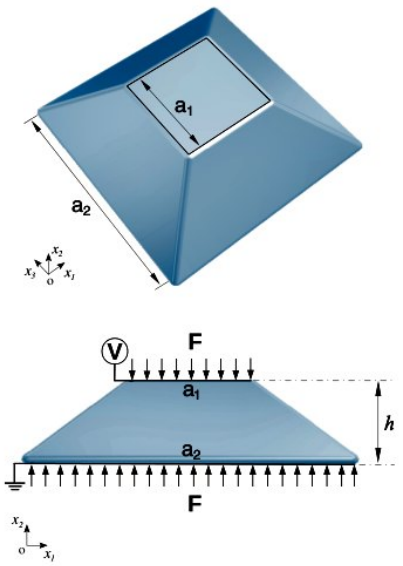

Figure 3: Truncated pyramid setup (Abdollahi et al., 2015).

Several different cases of truncated pyramids have been studied, varying the boundary conditions and the inclination angle of the pyramid. It has been found that for slim pyramids, where the inclination angle is large, the simplified analytical solution is close to the numerical coupled solution. Nonetheless, for plate pyramids with low values of the inclination angle, the analytical solution overestimates the flexoelectric coefficient μ_{1122}. It has also been proved that the lower is the inclination angle of the pyramid, the higher is the effective electromechanical coupling.

Therefore, in this second setup the transversal coefficient μ_{1122} is analyzed. The value of this coefficient is estimated to be between 1 and $100\,\mu C/m$ for BST (Zubko et al., 2013). This coefficient relates the flexoelectric response with polarization under compression, which induces a strain gradient on the pyramid.

2.3 Research on flexoelectricity under torsion

Research on the shear coefficient μ_{1212} is scarce at this moment. While the cantilever beam and the truncated pyramid are common and have been analyzed, there have not been many approaches to flexeoelectricity under torsion.

One of these few approaches is a recent experiment that has been carried out to develop a flexoelectric effect-based sensor for direct torque measurement (Zhang et al., 2013). This measurement mechanism does not require external electric power excitation and therefore noise is avoided, providing higher accuracy when measuring. Nonetheless, the shear coefficient μ_{1212} is not analyzed nor calculated.

3 Methodology

In this section, both analytical and numerical methods to obtain the flexoelectric effect under a shear strain gradient are described and implemented on a truncated cone. Finally, a comparison between both methods is developed to check whether the results are consistent or not.

The material that has been used for the development of the problem in this work is Barium Strontium Titanate (BST) in its nonpiezoelectric phase at room temperature. This material has cubic symmetry and is considered to be one of the strongest flexoelectric materials. BST is a ferroelectric material which behaves as a dielectric material for a range of values of the electric field, which means it has a certain electric coercivity.

3.1 Analytical method

It is not trivial to obtain a strain gradient when applying a load on a beam, especially under a shear strain. The geometry of the beam is essential to induce large strain gradients and of course large polarization. To simplify the problem, isotropic elasticity and permittivity are considered and cubic symmetry is adopted for the flexoelectric tensor. Therefore there are only two independent elastic constants, which are the Young's modulus E and the Poisson's ratio ν.

Probably the most simple geometry to work with is the cylinder. Thus, let us check if polarization is induced with this geometry first. According to (Miquel-Canet, 2012), for a cylindrical bar under uniform warping, the displacement field in Cartesian coordinates is:

$$u_1 = -\theta\, x_3\, x_2 \qquad u_2 = \theta\, x_3\, x_1 \qquad u_3 = \theta\, \varphi(x_1, x_2)\,, \tag{3}$$

where θ is the angle of twist and $\varphi(x_1, x_2)$ is a warping function to be determined and whose Laplacian is zero. Then, according to (Agelet and Oliver, 2000), the expression of the strain and its gradient can be written as:

$$\varepsilon_{ij} = \frac{1}{2}\left(\frac{\partial u_i}{\partial x_j} + \frac{\partial u_j}{\partial x_i}\right), \tag{4}$$

$$\frac{\partial \varepsilon_{ij}}{\partial x_l} = \frac{1}{2}\frac{\partial}{\partial x_l}\left(\frac{\partial u_i}{\partial x_j} + \frac{\partial u_j}{\partial x_i}\right), \tag{5}$$

and after applying Eq. (2), polarization becomes:

$$P_1 = 0 \qquad P_2 = 0 \qquad P_3 = \frac{\theta}{2} \triangle\varphi \; = 0. \tag{6}$$

Now it is proved that for a cylindrical bar under uniform warping, polarization is not induced. Thus, other conditions or geometries need to be explored.

A truncated cone is proposed as the second geometry to work on and check if the flexoelectric effect is induced. This cone is fixed on the larger base and is free on the smaller base, where a pure torque effort is applied. From now on, $x_1 = x$, $x_2 = y$ and $x_3 = z$.

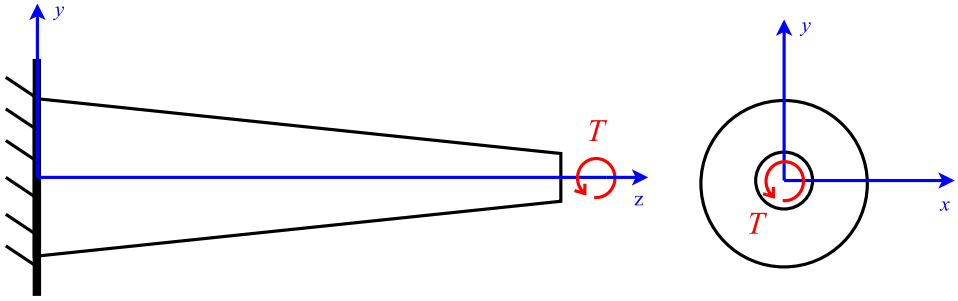

Figure 4: Schematic of the truncated cone and the applied torque.

For pure torsion, the angle of twist $\theta(z)$ of a continuously varying bar such as a truncated cone is:

$$\theta(z) = \int_0^z \frac{T}{G\,J(\alpha)}\,d\alpha\,, \tag{7}$$

where T is the torque applied and J is the polar moment of inertia which can vary along the z axis.

For the free end of the truncated cone, the prescribed angle of twist θ_L can be obtained after integrating Eq. (7) from 0 to L, as:

$$\theta_L = \frac{2\,T\,L}{3\,\pi\,G\,(r_0 - R_0)}\left(\frac{1}{R_0^3} - \frac{1}{r_0^3}\right). \tag{8}$$

Therefore the applied torque T can be obtained as:

$$T = \frac{3\,\theta_L\,\pi\,G\,(r_0 - R_0)}{2\,L\left(\frac{1}{R_0^3} - \frac{1}{r_0^3}\right)}\,. \tag{9}$$

The shear strain of the truncated cone under this torque can be expressed as:

$$\gamma(z) = r(z)\,\frac{\partial\,\theta(z)}{\partial\,z}\,, \tag{10}$$

where $r(z)$ is the radius of the cone, which varies along the z axis. Consequently, the shear strain gradient is obtained as:

$$\frac{\partial \gamma(z)}{\partial z} = \frac{\partial}{\partial z}\Big(r(z)\,\frac{\partial \phi(z)}{\partial z}\Big)\,. \tag{11}$$

After inserting Eq. (7) in Eq. (11) it is possible to derive the strain gradient function:

$$\frac{\partial \gamma(z)}{\partial z} = \frac{8\,T\,(R_0 - r_0)}{\pi\,G\,L}\Big(\frac{r_0 - R_0}{L}\,z + R_0\Big)^{-4}\,. \tag{12}$$

The strain gradient can be further expanded by substituting Eq. (9), which is the value of T, in Eq. (12).

$$\frac{\partial \gamma(z)}{\partial z} = \frac{12\,\theta_L\,(r_0 - R_0)^2}{L^2\left(\frac{1}{r_0^3} - \frac{1}{R_0^3}\right)}\Big(\frac{r_0 - R_0}{L}\,z + R_0\Big)^{-4}\,. \tag{13}$$

As Eq. (13) shows, the strain gradient is not zero for a truncated cone under the twist θ_L. In addition, it does not depend on the shear modulus of the material G. For a cylindrical bar, where the radius is constant, the strain gradient becomes zero, as previously proved.

According to Eq. (2), if the strain gradient is not zero, a certain polarization P is induced. This polarization is obtained as:

$$P(z) = \mu_{1212}\,\frac{\partial \gamma(z)}{\partial z}\,, \tag{14}$$

where $\mu_{1212} = 0.1\,\mu C/m^2$. The exact value of μ_{1212} is uncertain therefore an estimated value has been used. The other values characterizing the cone are presented in Table (2).

Property	**Symbol**	**Numerical value**
Larger base radius	R_0	263 nm
Smaller base radius	r_0	75 nm
Height	L	1 μm
Prescribed angle of twist	θ_L	0.075 rad
Young modulus	E	153 GPa
Poisson ratio	ν	0.333
Shear modulus	G	57.4 GPa

Table 2: Dimensions and properties of the truncated cone.

It is possible to see from Eq. (14) that the strain gradient varies along the z axis inducing a polarization due to flexoelectricity.

Figure (5) shows how polarization varies along the z axis, from 0 to L.

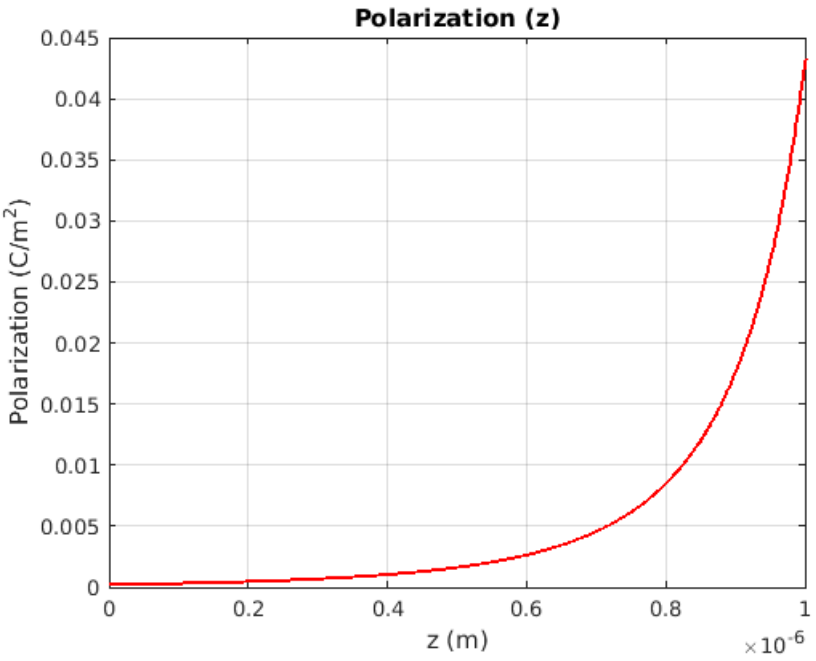

Figure 5: Polarization obtained using the data in Table (2) for the truncated cone.

The maximum value of the induced polarization according to the analytical results is:

$$P_{max,\,analytically} = 0.0434\, C/m^2\,. \tag{15}$$

Polarization is accumulated on the free end of the truncated cone and it decreases along the z axis, becoming zero on the fixed end of the truncated cone.

The elastic and the flexoelectric problems are not coupled in the analytical method. The strain gradient has been calculated according to the theory of elasticity and then introduced in the equation of flexoelectricity, without taking into account the effects that the polarization would produce on the strain gradient and viceversa. This is a simplification that has been introduced in order to obtain an approximate solution of the problem, therefore an error has been introduced by neglecting the coupling of both phenomena.

After evaluating the results of the numerical solution it will be possible to decide whether the analytical method under/overestimates the value of the polarization.

3.2 Numerical method

Analytical solutions can be derived for only the mechanical problem and for a few simple geometries such as the cylindrical bar or the truncated cone. Self-consistent numerical solutions of the flexoelectric governing equations are needed for an accurate estimation of the flexoelectric effect. Solving the coupled problem of flexoelectricity is essential to properly understand experiment measurements and, consequently, correctly estimating the flexoelectric coefficients. Indeed, as shown by (Abdollahi et al., 2014 and Abdollahi et al., 2015), estimating the strain gradients in common experimental setups from elasticity alone (thereby neglecting the electromechanical coupling) leads to over- or underestimation of the flexoelectric coefficients by several orders of magnitude. For this reason, the flexoelectric problem needs to be coupled and all calculations should be made as introduced in this section.

The constitutive equation for the electric polarization P in a linear dielectric solid which possesses flexoelectricity is:

$$P_i = \chi_{ij}\, E_j + \mu_{klij} \nabla_j\, \varepsilon_{kl}\,, \tag{16}$$

where the first term corresponds to the dielectric response and the second term corresponds to the flexoelectric effect. E is the electric field, ε is the mechanical strain and χ is the second-order dielectric susceptibility tensor.

The electric displacement D can be therefore expressed as:

$$D_i = \varepsilon_0\, E_i + P_i = \kappa_{ij}\, E_j + \mu_{klij}\, \nabla_j\, \varepsilon_{kl}\,, \tag{17}$$

where ε_0 is the permittivity of free space and κ_{ij} is the second order dielectric tensor. The electric field can be expressed as the derivative of the electric potential ϕ as $E_i = -\phi_{,i}$.

The constitutive equation for the mechanical stress σ is:

$$\sigma_{ij} = \mathbb{C}_{ijkl}\, \varepsilon_{kl} + \mu_{lijk}\, E_{l,k} - h_{ijklmn}\, \varepsilon_{lm,nk}\,, \tag{18}$$

where the first term is the elastic response, the second term is the converse flexoelectric effect and the third term is the strain-gradient elastic response. This last term is introduced for two reasons: firstly, for a physical purpose, because it enriches the continuum theory of elasticity extending its validity to nanoscales and secondly, for a computational purpose, because it stabilizes numerical solutions. $\mathbb{C}$ is the fourth-order tensor of elastic

moduli, ∇E is the electric field gradient and h is the sixth-order strain-gradient elasticity tensor.

Equations (17) and (18) are derived from the electromechanical enthalpy energy density for a linear flexoelectric solid, which can be written as:

$$\mathcal{H}(\varepsilon_{ij}, E_i, \varepsilon_{jk,l}) = \frac{1}{2}\,\mathbb{C}_{ijkl}\,\varepsilon_{ij}\,\varepsilon_{kl} - \mu_{ijkl}\,E_i\,\varepsilon_{jk,l} - \frac{1}{2}\,\kappa_{ij}\,E_i\,E_j + \frac{1}{2}\,h_{ijklmn}\,\varepsilon_{ij,k}\,\varepsilon_{lm,n}\,. \quad (19)$$

By minimizing Eq. (19) it is possible to obtain numerically the optimized values for the displacement field $\mathbf{u}$ and the electric potential field ϕ. Thus, any geometry can be analyzed to evaluate flexoelectricity and there is no need to use analytical methods. Nonetheless, note the presence of the second derivatives of the displacements in Eq. (19).

The problem analyzed in this work cannot be solved using traditional finite elements methods (FEM) because the strain gradient needs to be calculated and therefore second derivatives of the displacement field are needed. The reason is that FEM uses C^0 approximant functions but to solve this problem the approximant functions must be at least C^1. Figures (6) and (7) show a schematic of the problem.

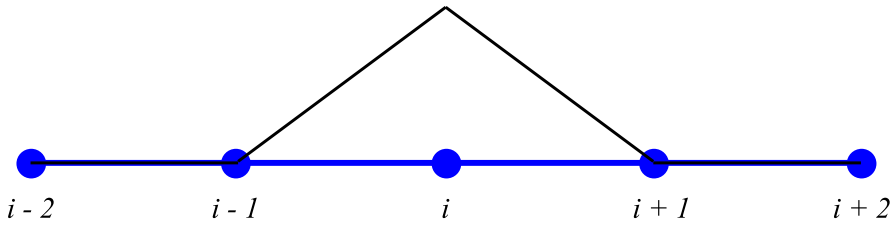

Figure 6: Example of approximant function for node i using traditional FEM.

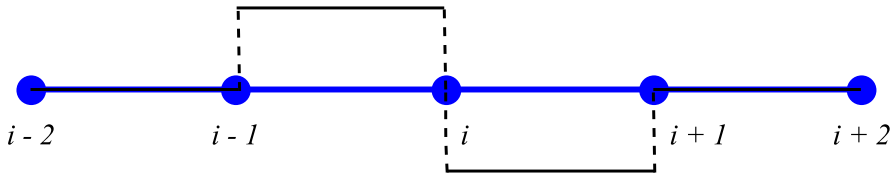

Figure 7: Example of the derivative of the approximant function for node i using traditional FEM.

A solution to this problem is to use smooth basis functions. These approximant functions are C^∞ and they are both continuous and derivable in the adjacent nodes.

In this work, the method that has been chosen to solve the presented problem is the *maximum - entropy* (*max-ent*) method (Arroyo and Ortiz, 2005). This method consists

on a one-parameter family of C^∞, smooth convex approximation schemes. These schemes can be used as a basis for the numerical solution of PDEs. Furthermore, it is proved that the accuracy of local *max-ent* approximation schemes is superior than the accuracy of FEM. This method allows to determine several smooth basis functions $p^\alpha(\mathbf{x})$ localized around its corresponding node. Figure (8) shows a schematic of these functions.

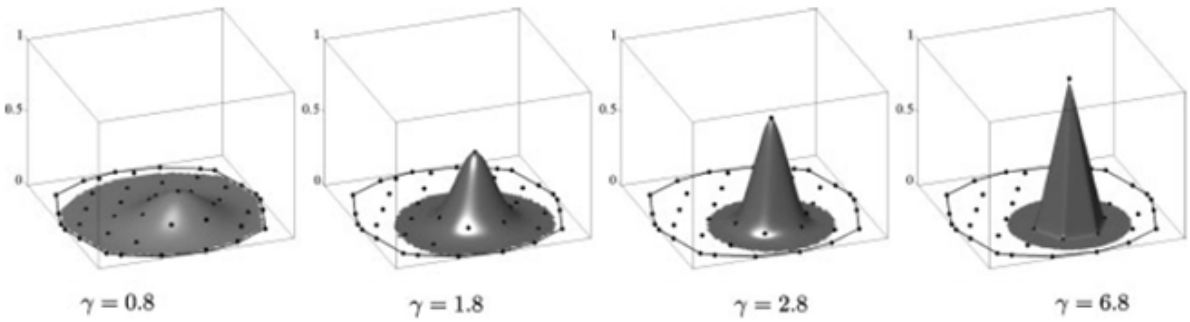

Figure 8: Example of smooth approximant functions. The γ parameter controls the locality of the function (Arroyo and Ortiz, 2005).

All terms in Eq. (19) need to be discretized in order to obtain a numerical solution. The discretized form of displacement field $\mathbf{u}$ and electric potential field ϕ are:

$$\mathbf{u}(\mathbf{x}) = \sum_{a=1}^{N} p^a(\mathbf{x})\,\mathbf{u}^a\,, \qquad \phi(\mathbf{x}) = \sum_{a=1}^{N} p^a(\mathbf{x})\,\phi^a\,. \tag{20}$$

From this point on, the arguments of the basis functions are omitted for simplicity, resulting $\mathbf{u} = \sum_{a=1}^{N} p^a \mathbf{u}^a$.

After introducing the discretized form of the displacement and electric potential fields as well as their respective derivatives in Eq. (19), the discrete representation of the total electromechanical entalpy becomes:

$$\begin{aligned} H(\mathbf{U},\phi) = &\frac{1}{2}\sum_{a,b}\mathbf{u}^{aT}\left(\int_\Omega \mathbf{B}_\mathbf{u}(p^a)\mathbb{C}\mathbf{B}_\mathbf{u}^T(p^b)d\Omega\right)\mathbf{u}^a + \sum_{a,b}\mathbf{u}^{aT}\left(\int_\Omega \mathbf{H}_\mathbf{u}(p^a)\mu^T\mathbf{B}_\phi^T(p^b)d\Omega\right)\phi^b \\ &+\frac{1}{2}\sum_{a,b}\left(\int_\Omega \mathbf{B}_\phi(p^a)\mathbf{K}\mathbf{B}_\phi^T(p^b)d\Omega\right)\phi^a\phi^b + \frac{1}{2}\sum_{a,b}\mathbf{u}^{aT}\left(\int_\Omega \mathbf{H}_\mathbf{s}(p^a)\mathbf{h}\mathbf{H}_\mathbf{s}^T(p^b)d\Omega\right)\mathbf{u}^a\,, \\ &-\sum_a\left(\int_{\Gamma_t}\bar{\mathbf{t}}p^a dS\right)\mathbf{u}^a + \sum_a\left(\int_{\Gamma_D}\omega p^a dS\right)\phi^a \end{aligned} \tag{21}$$

where $\bar{\mathbf{t}}$ are the imposed mechanical tractions and ω the prescribed change density. For more detail, see (Abdollahi et al., 2015).

From Eq. (21) the classic system of functions $\mathbf{K}\,x = \mathbf{f}$ can be solved, where the matrix $\mathbf{K}$ corresponds to the first four terms except for the continuum displacements $\mathbf{u}$ and the electric potential fields ϕ, which correspond to x. The last two terms of the equation correspond to the boundary conditions of the problem $\mathbf{f}$.

This numerical method is applied to the problem of the truncated cone with the same characteristics as the truncated cone in Section (3.1). Stress free boundary conditions have been chosen and the displacements along x, y and z axis as well as the electric potential are prescribed to be zero at the fixed end. The displacements and the electric potential are unknown at the free end.

Once the problem is solved and the electric potential is calculated at the free end, it is possible to obtain polarization as:

$$P = K\,E = -K\,\nabla\phi\,, \tag{22}$$

where P is the polarization, E is the electric field, ϕ is the electric potential and K is the dielectric constant of the Barium Strontium Titanate, whose value is $K = 0.885\,\mu C/(Vm^2)$.

Figure (9) shows the results of the simulation with numerical methods. The edges of the cone have been rounded to avoid unphyiscal singularities.

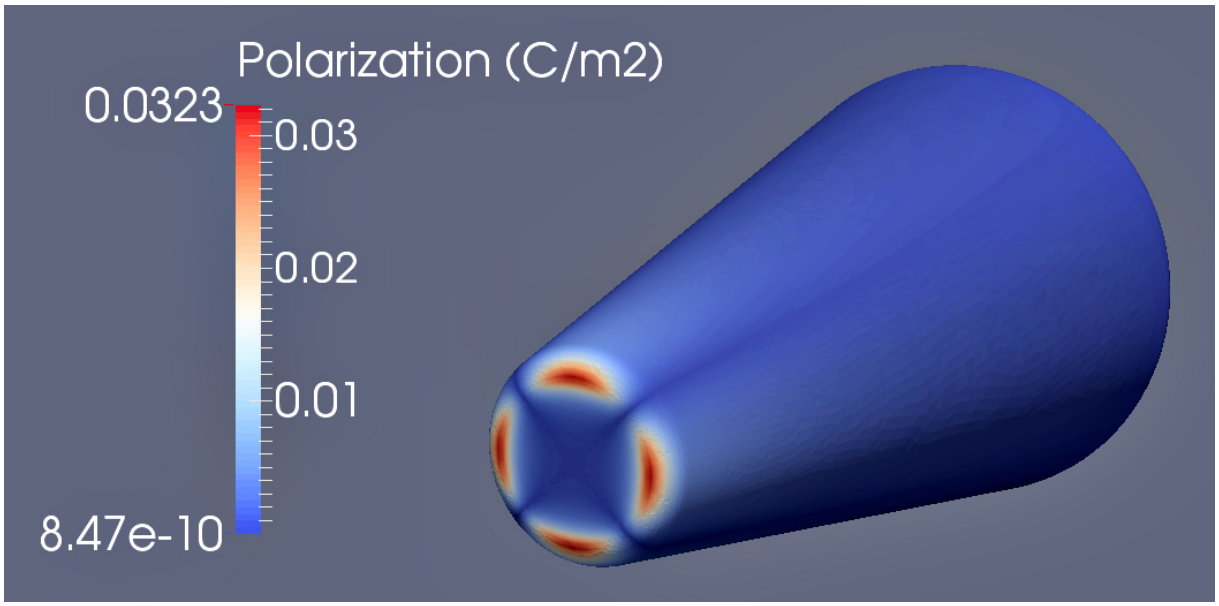

Figure 9: Numerical simulation results.

Therefore, the maximum value of the induced polarization is:

$$P_{max,\,numerically} = 0.0323\,C/m^2\,. \tag{23}$$

As in Section (3.1), polarization is focused on the free end of the truncated cone and it decreases along the z axis, becoming zero on the fixed end of the truncated cone.

3.3 Consistency of the methods

It is essential to understand the importance of coupling strain gradient and polarization when solving the flexoelectricity problem. If this coupling is not correctly introduced, an error is produced. Nonetheless, in some cases this error is small and therefore the uncoupled problem can be solved with an acceptable accuracy.

On the one hand, the problem has been solved uncoupled following the analytical method and the maximum value of the polarization is obtained as:

$$P_{max,\,analytically} = 0.0434\, C/m^2\,.$$

On the other hand, the problem has been solved coupled following the numerical method and the maximum value of the polarization is calculated as:

$$P_{max,\,numerically} = 0.0323\, C/m^2\,.$$

After analyzing both solutions, it is clear that they are not identical because an approximation error has been produced. Nevertheless, they are comparable and in the same order of magnitude. Furthermore, polarization is accumulated on the free end and its value decreases along the z axis, becoming zero at the fixed end.

These results show the consistency of both methods. Despite this small difference, the numerical method results in a reasonable solution. Therefore, other geometries can be analyzed and compared regarding the flexoelectric response.

4 Results and discussion

In Section (3) both the analytical and the numerical methods have been studied and compared for a truncated cone. In this section, other geometries are presentend and the values of the polarization are obtained according to several numerical simulations using the *max-ent* scheme. This will help to determine what geometries are optimal to induce the highest value of polarization and to solve the problem from other perspectives in which several difficulties may arise.

4.1 Truncated cone #1

In this section, the results from the first simulation are compiled. The properties of this truncated cone are the same properties as the cone analyzed in Section (3.2). These properties are presented in Table (2), with $R_0 = 263\,nm$ and $r_0 = 75\,nm$.

The maximum value of the induced polarization for the truncated cone #1 according to the simulation is:

$$P_{max\,numerically,\,truncated\,cone\,\#1} = 0.0323\,C/m^2\,. \tag{24}$$

Figure (10) shows the results of the simulation:

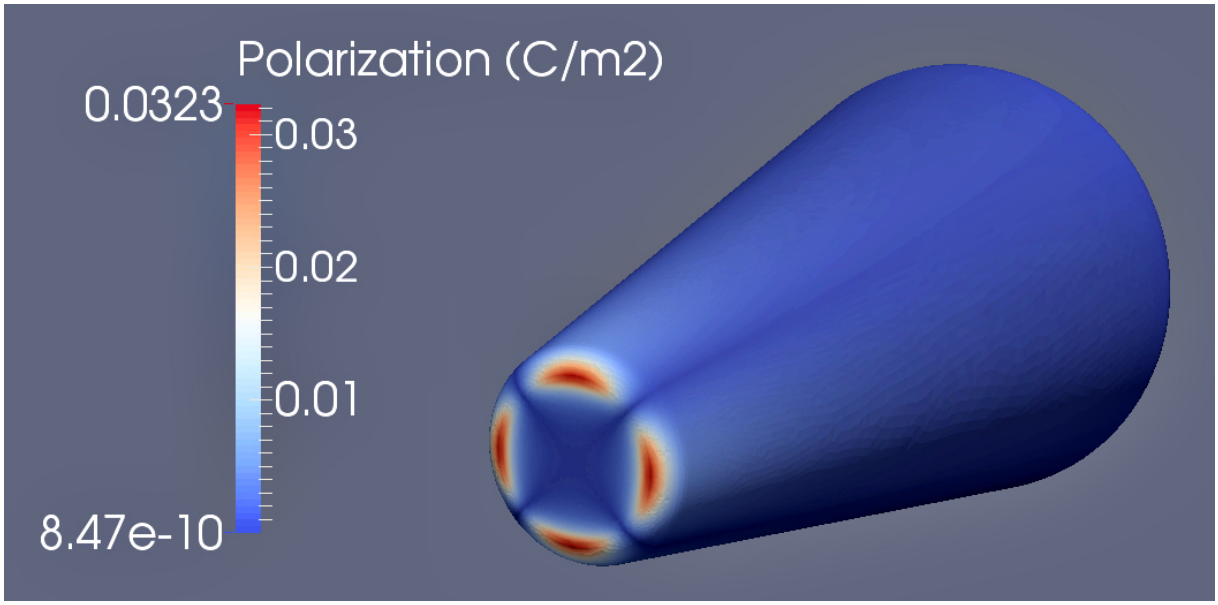

Figure 10: Numerical simulation results for the truncated cone #1.

The maximum value of the induced polarization for the truncated cone #1 according to the analytical method is:

$$P_{max\,analytically,\,truncated\,cone\,\#1} = 0.0434\,C/m^2\,. \tag{25}$$

Thus, as stated in Section (3.3), both solutions are comparable and the uncoupled analytical problem is accurate enough.

4.2 Truncated cone #2

The properties of the truncated cone #2 are exactly the same as those for the truncated cone #1 except for the radii. For the truncated cone #2, $R_0 = 932\,nm$ and $r_0 = 87\,nm$, which results in a fatter cone.

The maximum value of the induced polarization for the truncated cone #2 according to the simulation is:

$$P_{max\,numerically,\,truncated\,cone\,\#2} = 0.0745\,C/m^2\,. \tag{26}$$

Figure (11) shows the results of the simulation:

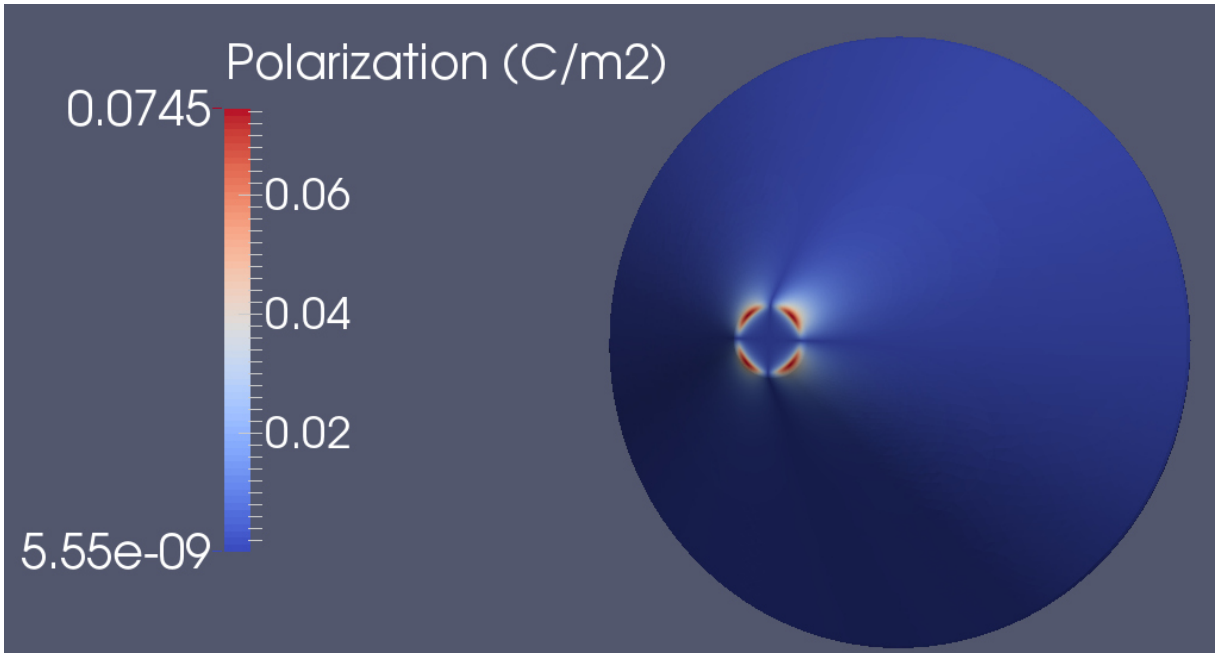

Figure 11: Numerical simulation results for the truncated cone #2.

Nevertheless, the maximum value of the induced polarization for the truncated cone #2 according to the analytical method is:

$$P_{max\,analytically,\,truncated\,cone\,\#2} = 0.7392\,C/m^2\,. \tag{27}$$

This new ratio R_0/r_0 of the radii makes the cone much fatter and therefore the effects of the strain gradient on the polarization are different from the previous cone. The maximum value of the polarization is larger for the truncated cone #2 than the truncated cone #1 in both analytical and numerical results. However, there is a divergence between the analytical and the numerical results. In fact, the value of the polarization is overestimated in the analytical solution, being ten times larger for the truncated cone #2.

This difference shows the importance of numerical methods when solving a complex problem such as the flexoelectric coupled problem. For certain geometries, the simplifications made in the analytical problem do not have a strong incidence in the final result, as in the truncated cone #1. Surprisingly, for another cone with different dimensions, such as the truncated cone #2, the analytical solution does not make any sense because the error due to simplifications is too large.

A similar situation was detected in (Abdollahi et al., 2015) for truncated pyramids under compression loads, as explained in Section (2.2). For high values of the inclination angles, both numerical and analytical solution are similar, whereas for low values of the inclination angle, the analytical method overestimates the results.

4.3 Truncated pyramid

Pyramids behave slightly different than cones under torsion. To determine this behaviour, a truncated pyramid is studied. The problem analyzed with this pyramid is exactly the same as the problem for the truncated cone except for the geometry of the nanobeam. For the truncated pyramid, $D_0 = 332\,nm$ and $d_0 = 146\,nm$, where D_0 corresponds to the side of the larger base and d_0 corresponds to the side of the smaller base of the truncated pyramid.

For the truncated pyramid problem, only the numerical solution has been considered. In fact, numerical methods and simulations are thought to work as a tool for solving complex problems and geometries, skipping all the analytical proceedings and providing the users

with high accuracy and a wide variety of geometries to work on, such as this truncated pyramid.

The maximum value of the induced polarization for the truncated pyramid according to the numerical method is:

$$P_{max\,numerically,\,truncated\,pyramid} = 0.0143\,C/m^2\,. \tag{28}$$

Figure (12) shows the results of the simulation:

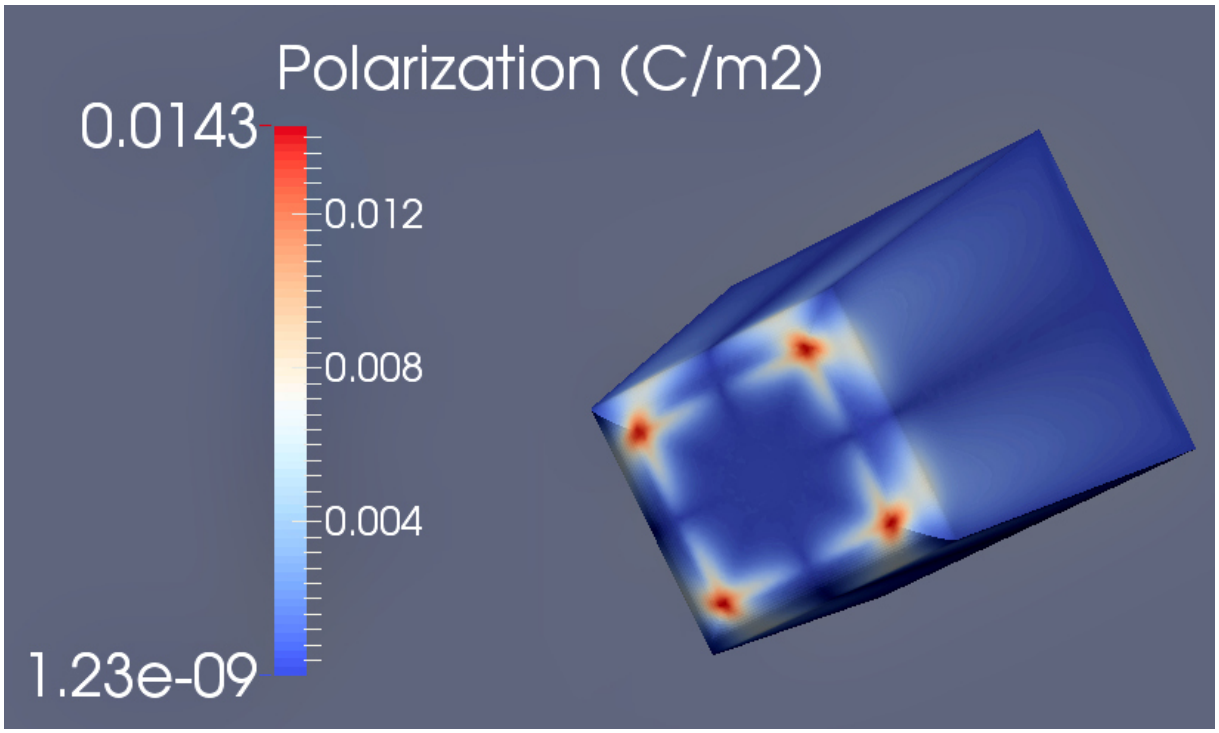

Figure 12: Numerical simulation results for the truncated pyramid.

It is clear that the value of the polarization obtained for the truncated pyramid is considerably smaller than for the truncated cones, being almost three times smaller than for the truncated cone #1 and seven times smaller than for the truncated cone #2.

4.4 Optimal geometry

The main goal of this work is to obtain large values of polarization when a torque is applied on a nanobeam. Thus, the optimal configuration of the beam should produce the highest possible value of polarization. This is essential when developing an experiment because low values of polarization are impossible to measure with the available tools.

The properties of the material have an important influence on the results of the polarization. For materials whose flexoelectric coefficient μ is large, it is easier to measure polarization. It has been found that dielectric materials such as ferroelectrics have large values of μ (Ma and Cross, 2006). The flexoelectric effect could enhance the ferroelectric effect and produce higher values of polarization when both phenomena are induced.

According to the results in Sections (4.1), (4.2) and (4.3), the optimal configuration would be the fatter truncated cone because it induces the maximum value of polarization, resulting twice the polarization for the slimmer cone. The value of the polarization obtained for the truncated cone #2 is measurable with the available technological tools. The truncated pyramid induces a low value of polarization and therefore it is not a recommended configuration for an experiment. Nonetheless, other geometries should be explored in order to obtain the optimal configuration and carry out a hypotethic experiment successfully.

5 Summary, conclusions and directions of future work

Several important conclusions related to flexoelectricity in nanobeams under torsion have derived from this work. These conclusions lead to several directions of future work which could complement the reasearch developed in the present work.

5.1 Summary and conclusions

The main conclusions derived from this work are:

i **An electromechanical coupling different from piezoelectricity has gained popularity in the last years: flexoelectricity.** Flexoelectricity relates polarization and strain gradient and it is proved to be relevant in nanoscale systems for any dielectric, whereas in piezoelectricity polarization can be obtained from an homogeneous deformation in macroscale systems, but only for non-centrosymmetric materials. Although there are many recent flexoelectricity studies, the accurate characterization of the phenomenon is in process and there is still a lot to discover. This work has contributed to the development of flexoelectricity focusing on nanobeams under torsion.

ii **Torsion can induce a shear strain gradient on several geometries to obtain polarization.** The strain gradient induced by a torque applied on the free end of a cylinder has been calculated using the theory of elasticity and the result has been zero. Then, the same problem has been solved with a truncated cone and a certain non-zero value of the strain gradient has been obtained. Then, this value has been introduced in the fundamental flexoelectric expression. Nonetheless, an error is produced when polarization and strain gradient are solved separately and not coupled in the problem. A certain value of polarization has been obtained using analytical methods and an error has been produced and assumed.

iii **Smooth functions are used to solve the flexoelectric problem numerically.** Working with strain gradients, i.e. the second derivative of the displacement field is not trivial when using numerical methods. The need of computing second derivatives makes traditional finite element methods useless and therefore other methodologies must be considered to solve the problem. In this work, smooth functions from the *max-ent* scheme are used to obtain the results. The problem of flexoelectricity can be solved with all the terms coupled from the electromechanical enthalpy energy density,

providing better accuracy to the solution. A certain value has been obtained using a numerical simulation.

iv **The results of both analytical and numerical methods have been discussed.** Despite an error is committed in the analytical method, both results are comparable. Thus, the numerical method is considered to be an accurate tool to obtain a solution from any type of beam geometry.

v **Several geometries have been compared using numerical simulations in order to maximize polarization.** Two different truncated cones and a truncated pyramid have been studied. Polarization reaches its maximum value at the free end of all geometries, where the torque is applied, and decreases until the value of zero at the fixed end. For the fatter truncated cone, the analytical method overestimates the value of the polarization, being ten times larger than the numerical method. The maximum value of polarization has been obtained from the fatter truncated cone, being almost three times larger than for the slimmer truncated cone and seven times larger than the truncated pyramid, all of them obtained numerically. This makes the fatter truncated cone an ideal candidate for experimental configuration.

5.2 Directions of future work

The work carried out in this study also leaves some open research lines for the future. The following lines are suggested:

i **Detecting what factors induce an error of one order of magnitude between the results of polarization in the analytical and the numerical methods for the fatter truncated cone.** While for the slimmer cone the analytical and numerical solutions are similar, in the fatter cone the difference is abrupt. Try to measure the impact of these factors and establish in which conditions the solution for the uncoupled problem is accurate.

ii **Understanding why the maximum values of polarization are located in subdomains of the base of the truncated cones and the truncated pyramid.** This polarization should change from zero to its maximum value in the θ direction, which means that for a certain angle both the zero and the maximum value collapse. From a mathematical point of view this is not possible and therefore the simulation

is forced to create four domains where polarization is maximum and four domain walls between these domains where polarization reaches its minimum value. Try to distinguish what factors induce these subdomains and why there are always four of them in truncated cones as well as in truncated pyramids.

iii **Exploring new geometries apart from those analyzed in this work to maximize polarization.** To configure a fully optimized experiment more geometries need to be studied and solutions must be as accurate as possible, with very fine meshes. With large values of polarization an experiment could be carried out and therefore the shear flexoelectric coefficient μ_{1212} could be estimated.

References

A. Abdollahi. *Phase-field modeling of fracture in ferroelectric materials*. PhD thesis, Universitat Politècnica de Catalunya, Departament de Matemàtica Aplicada III, 2012.

A. Abdollahi, D. Millán, C. Peco, M. Arroyo, and I. Arias. Computational evaluation of the flexoelectric effect in dielectric solids. *Journal of Applied Physics*, 116(093502), 2014.

A. Abdollahi, D. Millán, C. Peco, M. Arroyo, and I. Arias. Revisiting pyramid compression to quantify flexoelectricity: A three-dimensional simulation study. *Physical Review*, 91: 103104, 2015.

C. Agelet and X. Oliver. *Mecánica de Medios Continuos*. Edicions UPC, 2000.

M. Arroyo and M. Ortiz. Local maximum-entropy approximation schemes: a seamless bridge between finite elements and meshree methods. *International Journal for Numerical Methods in Engineering*, 65:2167–2202, 2005.

E. L. Cross. Flexoelectric effects: Charge separation in insulating solids subjected to elastic strain gradients. *Journal of Materials Science*, 41(1):53–63, 2006.

J. Hong and D. Vanderbilt. First-principles theory of frozen-ion flexoelectricity. *Phys. Rev. B*, 84:180101, 2011.

S. V. Kalinin and V. Meunier. Electronic flexoelectricity in low-dimensional systems. *Phys. Rev. B*, 77:033403, 2008.

S. V. Kalinin, S. Jesse, W. Liu, and A. A. Balandin. Evidence for possible flexoelectricity in tobacco mosaic viruses used as nanotemplates. *Applied Physics Letters*, 88(15), 2006.

S. M. Kogan. Piezoelectric effect during inhomogeneous deformation and acoustic scattering of carriers in crystals. *Sov.Phys.Solid State*, 5(10), 1964.

W. Ma and E. L. Cross. Flexoelectricity of barium titanate. *Applied Physics Letters*, 88 (23), 2006.

J. Miquel-Canet. *Resistencia de Materiales y Estructuras*. Ediciones CIMNE, 2012.

T. D. Nguyen, S. Mao, Y.-W. Yeh, P. K. Purohit, and M. C. McAlpine. Nanoscale flexoelectricity. *Advanced Materials (Weinheim, Germany)*, 25:946–974, 2013.

A. G. Petrov. Flexoelectric model for active transport. *Physical and Chemical Bases of Biological Information Transfer*, page 111, 1975.

A. G. Petrov. Flexoelectricity of model and living membranes. *Biochimica et Biophysica Acta (BBA) - Biomembranes*, 1561(1):1 – 25, 2002.

R. Resta. Towards a bulk theory of flexoelectricity. *Phys. Rev. Lett.*, 105:127601, 2010.

I. S. Sokolnikoff. *Mathematical Theory of Elasticity*. Tata McGraw Hill Publishing Company Ltd., 1948.

A. K. Tagantsev. Piezoelectricity and flexoelectricity in crystalline dielectrics. *Phys. Rev. B*, 34:5883–5889, 1986.

S. Zhang, M. Xu, K. Liu, and S. Shen. A flexoelectricity effect-based sensor for direct torque measurement. *Journal of Physics D: Applied Physics*, 48:485502, 2013.

W. Zhu, J. Y. Fu, N. Li, and L. Cross. Piezoelectric composite based on the enhanced flexoelectric effects. *Applied Physics Letters*, 89(19), 2006.

P. Zubko, G. Catalan, A. Buckley, P. R. L. Welche, and J. F. Scott. Strain-gradient-induced polarization in $SrTiO_3$ single crystals. *Phys. Rev. Lett.*, 99:167601, 2007.

P. Zubko, G. Catalan, and A. K. Tagantsev. Flexoelectric effect in solids. *Annual Review of Materials Research*, 43, 2013.